Journal of Photonics for Energy

PhotonicsforEnergy.SPIEDigitalLibrary.org

# Responsivity and resonant properties of dipole, bowtie, and spiral Seebeck nanoantennas

Brhayllan Mora-Ventura
Ramón Díaz de León
Guillermo García-Torales
Jorge L. Flores
Javier Alda
Francisco J. González

SPIE.

Brhayllan Mora-Ventura, Ramón Díaz de León, Guillermo García-Torales, Jorge L. Flores, Javier Alda, Francisco J. González, "Responsivity and resonant properties of dipole, bowtie, and spiral Seebeck nanoantennas," *J. Photon. Energy* **6**(2), 024501 (2016), doi: 10.1117/1.JPE.6.024501.

# Responsivity and resonant properties of dipole, bowtie, and spiral Seebeck nanoantennas

**Brhayllan Mora-Ventura,[a] Ramón Díaz de León,[b] Guillermo García-Torales,[a] Jorge L. Flores,[a] Javier Alda,[c] and Francisco J. González[b,*]**

[a]Universidad de Guadalajara, Av. Revolución No. 1500, Guadalajara, Jal. 44430, México
[b]Universidad Autónoma de San Luis Potosí, Sierra Leona 550, Lomas 2da Sección, San Luis Potosí 78210, México
[c]University Complutense of Madrid, School of Optics, Arcos de Jalón 118, Madrid 28037, Spain

**Abstract.** Seebeck nanoantennas, which are based on the thermoelectric effect, have been proposed for electromagnetic energy harvesting and infrared detection. The responsivity and frequency dependence of three types of Seebeck nanoantennas is obtained by electromagnetic simulation for different materials. Results show that the square spiral antenna has the widest bandwidth and the highest induced current of the three analyzed geometries. However, the geometry that presented the highest temperature gradient was the bowtie antenna, which favors the thermoelectric effect in a Seebeck nanoantenna. The results also show that these types of devices can present a voltage responsivity as high as 36 $\mu$V/W for titanium–nickel dipoles resonant at far-infrared wavelengths.  [DOI: 10.1117/1.JPE.6.024501]

**Keywords:** Seebeck nanoantennas; thermoelectric nanoantennas; solar energy harvesting.

Paper 16008P received Jan. 24, 2016; accepted for publication Apr. 12, 2016; published online May 2, 2016.

## 1 Introduction

Optical antennas and resonant structures provide electrical field enhancement that can be used in several nanophotonic applications.[1,2] These types of devices have been used in several fields of science and technology due to their advantages in terms of polarization sensitivity, tunability, directionality, and small footprint.[3]

In the last decade, thermoelectric or Seebeck nanoantennas have been proposed as potential solar energy harvesters due to their tunability and the possibility of harvesting the electromagnetic portion of the solar spectrum, which cannot be converted into electrical energy through current photovoltaic technology.[4,5] The theory of operation of Seebeck nanoantennas consists of converting thermal energy induced by Joule heating in the nanoantenna into electrical energy by generating a voltage proportional to the difference in temperature between hot and cold bimetallic junctions.[4] Numerical simulation predicts that this technology can harvest solar energy with a higher efficiency than direct rectifiers coupled to optical antennas.[6] Also single-metal Seebeck nanoantennas have been proposed, which would simplify the fabrication process and allow the large-scale production of these devices using fabrication technologies such as nanoimprint lithography.[5,7]

Even though there have been numerous reports on the design and characterization of thermoelectric nanoantennas by several groups, a key figure of merit for these types of devices, the responsivity, has not been reported yet. In this work, a numerical evaluation and comparison of the responsivity for three types of Seebeck nanoantennas using different materials and geometries is presented.

*Address all correspondence to: Francisco J. González, E-mail: javier.gonzalez@uaslp.mx

In Sec. 2, we briefly describe the method and procedure used to evaluate the response of Seebeck nanoantennas. Section 3 presents the main results regarding geometrical and material parameters, including a useful comparison between the proposed cases. Finally, Sec. 4 summarizes the main conclusions of the paper.

## 2 Method

The induced current in the nanoantennas was calculated using finite element simulations. These types of simulations have been used successfully in several nanophotonic applications, including the evaluation of the performance and capabilities of Seebeck nanoantennas.[4,6] The analysis was made using a multiphysics approach by solving electromagnetic and heat transfer equations in order to obtain the increase in temperature due to electromagnetic incident energy. COMSOL Multiphysics, commercial software that solves partial differential equations using the finite element method, was used in this work due to the possibility of combining several physical effects in the same simulation. The numerical simulation procedure consisted of performing first an electromagnetic simulation in order to obtain the induced current across the antenna structure. Using the multiphysics capabilities of COMSOL, the obtained induced current was used as a Joule heating source in order to calculate the temperature in the antenna structure. Heat transfer is commonly described by three mechanisms: radiation, convection, and conduction. In our case, radiation is considered negligible because of the small temperature difference produced by the incoming wavefront.[8] Convection is also not considered as far as our analysis has been done in vacuum. Therefore, only conduction is taken into account, as has been done to model similar devices.[9]

The open circuit voltage of the Seebeck nanoantenna can be obtained as[4]

$$V_{\mathrm{oc}} = (S_A - S_B)\Delta T, \tag{1}$$

where $\Delta T$ is the difference in temperature between the center (hot spot) and the open ends of the antenna (cold spots) where the minimum temperature is located, and $S_A$ and $S_B$ are the Seebeck coefficients of the metals used.

The electromagnetic simulation was performed by launching a linearly polarized electromagnetic plane wave with a polarization state matching the polarization of the antenna, and considering the antenna structure at vacuum. The electric field amplitude of the plane wave is set at a specific value, and the induced current in the antenna as a function of the plane wave's frequency is evaluated by integrating the current density over the cross-section of the antenna at its feed point, where this current density reaches its maximum value at the resonant wavelength.

The optical properties of materials used for the simulations were obtained from data reported in the literature and take into account the dispersion at the frequencies simulated.[10,11]

## 3 Results

In this section, the response of different types of Seebeck nanoantennas is evaluated. First, a simple dipole geometry is used to calculate the induced current as a function of frequency and the length of the dipole structure. Then, the results are compared to the theoretical resonance predicted by classical antenna theory. In a second series of simulations, a parametric study with different materials commonly used in Seebeck nanoantennas is performed for a resonant dipole antenna, and finally, a comparison between three different geometries of optical antennas (dipole, bowtie, and square spiral) is presented. These results can be used to obtain an optimized design of Seebeck nanoantennas.

An estimation of the responsivity of these devices is reported using the experimentally obtained collection area of these types of antennas.[12]

### 3.1 *Dipole Length Study*

For comparison purposes, the response of a gold dipole antenna as a function of frequency is analyzed for different dipole lengths (Fig. 1). Results show that the deviation from the expected

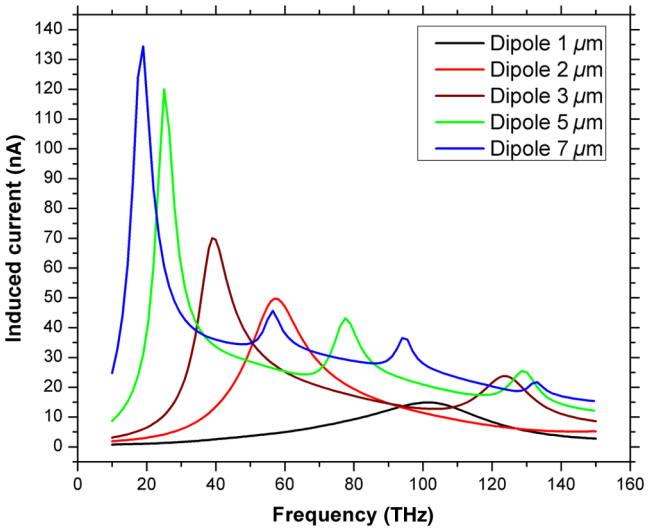


**Fig. 1** Induced current as a function of frequency for gold dipoles with different lengths.

resonant frequency from classical antenna theory increases with frequency. This happens due to the increase in the resistivity of gold at optical frequencies; this effect also allows the electromagnetic wave to penetrate within the resonant structure. This effect can also be modeled using an effective length for the resonant dipole.[13]

Table 1 shows the calculated resonant wavelength for five different dipole lengths. The resonant frequency was obtained by calculating the frequency at which the maximum current was induced in the whole dipole structure. The current responsivity was calculated as the ratio of the induced current and the optical power incident on the antenna. The optical power was obtained as the product of the irradiance and the receiving area of the antenna, which can be approximated by the resonant wavelength squared ($\lambda_{res}^2$), according to the experimental measurements.[14]

This discrepancy in the optimum length of the dipole for a given wavelength is of importance when designing resonant elements at infrared and visible frequencies. This scaling factor has to be revised when considering the effect of the substrate on the resonance of the element. When Seebeck nanoantennas are designed to scavenge thermal radiation coming from moderate temperature radiators (thermal engines, intercoolers, and so on), the temperature of the radiating element fixes the optimum wavelength of operation through the Wien displacement law: $\lambda_{max}T = 2898\ \mu$m·K. Therefore, this parametric study allows us to select the optimum dipole length for a given radiation temperature. When considering the resonant wavelength given in Table 1, we find that thermal radiator temperature ranges from room temperature to 760°C.

## 3.2 *Effect of Materials*

In the case of Seebeck nanoantennas, the chosen materials affect the responsivity in two ways, the first due to the Seebeck coefficient of the materials used and the second by the ability of the

**Table 1** Shift in resonance and current responsivity for different gold dipole lengths.

| Dipole length ($\mu$m) | Resonant wavelength ($\mu$m) | Resonant shift from theory ($\lambda/2$) | Induced current (nA) | Current responsivity (nA/W) |
|---|---|---|---|---|
| 1 | 2.9 | 45% | 14.9 | 328.83 |
| 2 | 5.2 | 30% | 49.7 | 611.69 |
| 3 | 7.6 | 27% | 70.0 | 589.47 |
| 5 | 12 | 20% | 119.9 | 639.47 |
| 7 | 15 | 7% | 134.4 | 573.44 |

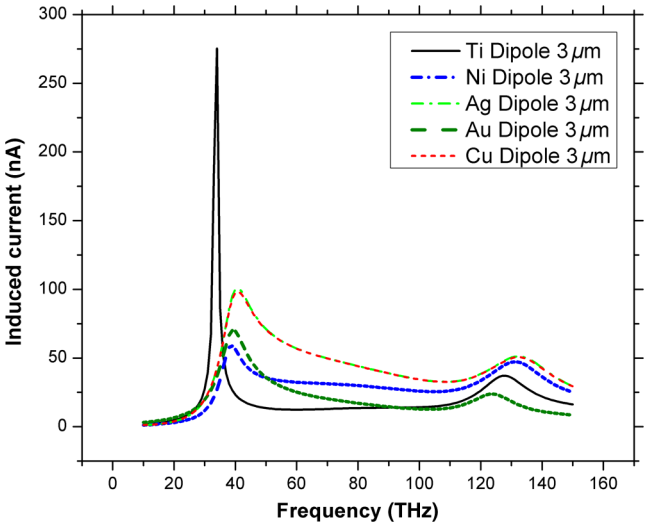


**Fig. 2** Induced current by a linearly polarized plane wave on gold, copper, silver, titanium, and nickel dipoles as a function of frequency.

material to induce currents due to the radiant flux incident on the nanoantenna. A parametric study involving different metals and a single dipole geometry was performed (see Fig. 2). In this case, the length of the dipole was fixed at 3 $\mu$m, and several simulations were performed using different materials.

Table 2 shows the resonant wavelength and current responsivity of a 3-$\mu$m dipole for five different materials. In this table, we see that the resonant wavelength varies according to the optical properties of the material used for the fabrication of the antenna, and therefore its responsivity. Again, an appropriate selection of materials is of importance to optimize the signal obtained from a Seebeck nanoantenna.

### 3.3 *Analysis of Different Antenna Geometries*

Several geometries can be used for fabricating Seebeck nanoantennas. Their performance is strongly related to their dimensions and how the electric field and currents are generated. The final choice of the geometry will be related to the desired polarization selectivity and the level of the signal obtained from each geometry.

Figure 3 shows the induced current density for three different types of nanoantennas. From these results, we can see that the bowtie and square spiral nanoantennas show the highest induced current density in comparison with the dipole nanoantennas. Also, in Fig. 3, we can see how the bowtie configuration concentrates most of the induced current in the feed of the antenna, leaving the ends of the antenna arms almost without current. This uneven current distribution favors the Seebeck effect by concentrating the heat generated by

**Table 2** Resonance and responsivity of a 3-$\mu$m dipole for different materials.

| Materials | Resonant wavelength ($\mu$m) | Resonant shift from theory ($\lambda/2$) | Induced current (nA) | Current responsivity (nA/W) |
|---|---|---|---|---|
| Au | 7.6 | 26.5% | 70 | 589.47 |
| Ag | 7.3 | 20% | 101.0 | 850.53 |
| Cu | 7.3 | 20% | 98.6 | 830.32 |
| Ti | 8.82 | 47% | 275.5 | 2320.00 |
| Ni | 7.6 | 26.5% | 58.8 | 495.1 |

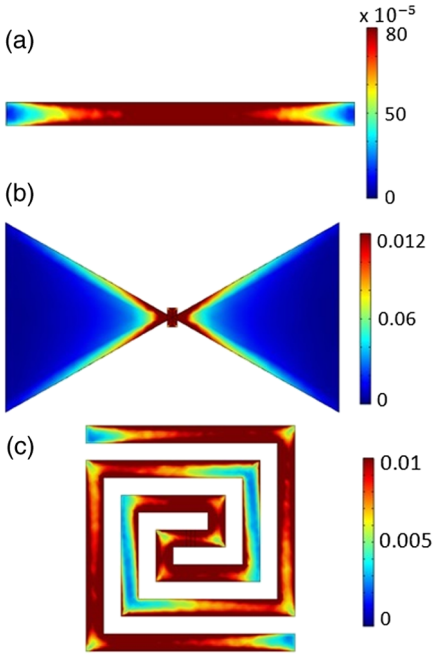


**Fig. 3** Induced current density ($A/m^2$) due to an incident plane wave on a (a) dipole nanoantenna, (b) bowtie nanoantenna, and (c) square spiral nanoantenna.

Joule heating in a small area, where the hot terminal can be placed, and a region without current where the cold terminal could be placed.

Table 3 shows the total induced current in the antenna for the three different geometries and the current responsivity taken as the induced current divided by the incident optical power.

Figure 4 shows the induced current for the three geometries considered as a function of the frequency of the incident plane wave. From Fig. 4, it can be seen that the square spiral configuration has the widest bandwidth and the highest induced current of the three geometries. However, Fig. 3 shows that the geometry that can generate a higher temperature gradient is the bowtie geometry, which favors the thermoelectric effect in a Seebeck nanoantenna.

### 3.4 *Thermal Analysis and Seebeck Responsivity*

Once we have analyzed the role of the geometry, material, and shape in the response of optical antennas, we combine different metals in order to obtain their thermal response when the resonant structure is illuminated under optimum conditions. As we know, the key factor in Seebeck nanoantennas is the difference in temperature between the hot and cold junctions. In this section, we will pay special attention to the analysis of bimetallic antennas and their thermal behavior when a given irradiance is impinging on them. Therefore, an analysis of the best bimetal combination is necessary to propose the fabrication of devices.

**Table 3** Resonant frequency, induced current, and current responsivity for different antenna geometries.

| Geometry | Resonant frequency (THz) | Resonant wavelength ($\mu$m) | Induced current (nA) | Current responsivity (nA/W) |
|---|---|---|---|---|
| Dipole | 39 | 7.6 | 70.0 | 589.47 |
| Triangular | 31 | 9.6 | 146.1 | 974.00 |
| Square spiral | 25 | 12 | 520.6 | 2776.53 |

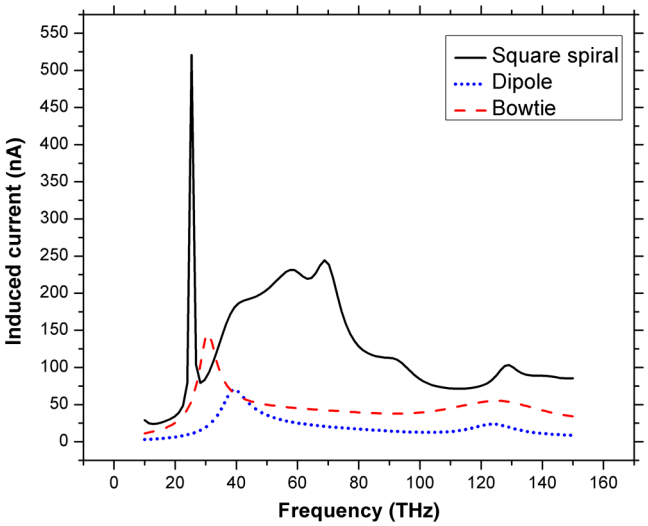


**Fig. 4** Induced current by a linearly polarized plane wave on gold dipole, bowtie, and square spiral nanoantennas as a function of frequency.

Even though from the previous section, we see that the bowtie geometry is the one that generates a higher temperature gradient and would be the ideal geometry to enhance the thermoelectric effect on Seebeck nanoantennas, the material analysis was made with dipole antennas due to the simplicity of the simulations and the fact that the results obtained with these geometries would apply to any geometry.

Figure 5 shows the temperature increase as a function of the length of the antenna structure for different combinations of materials. Nickel was always chosen as one of the materials since it is the only one that has a negative Seebeck coefficient. Therefore, this material combined with another with a positive Seebeck coefficient would give the highest voltage output [Eq. (1)].

Table 4 shows the difference in temperature calculated between the bimetallic junction and the open ends of the dipole antenna. The voltage response of the antenna was evaluated by using the Seebeck effect. The Seebeck coefficients were taken as bulk ($S_{Ag} = S_{Au} = S_{Cu} = 6.5\ \mu V/K$, $S_{Ti} = 7.2\ \mu V/K$, and $S_{Ni} = -15\ \mu V/K$). Table 4 also shows the voltage responsivity of the Seebeck nanoantennas. The values given in Table 4 can be used to make a first-order approximation of the efficiency of these devices calculated as the power that can be extracted by a current flowing through the antenna due to a voltage

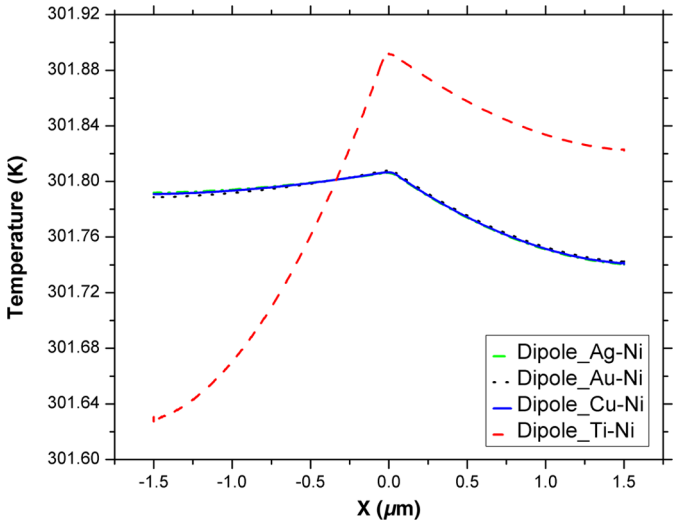


**Fig. 5** Distribution of temperature across the dipole nanoantennas for different metals analyzed in this work.

**Table 4** Difference temperature and voltage responsivity for Seebeck dipole nanoantennas with 3-$\mu$m length.

| Material junction | $\Delta T$ (K) | $V_{oc}$ ($\mu$V) | Voltage responsivity ($\mu$V/W) |
|---|---|---|---|
| Ag-Ni | 0.051 | 1.096 | 9.23 |
| Au-Ni | 0.046 | 0.989 | 8.32 |
| Cu-Ni | 0.049 | 1.036 | 8.72 |
| Ti-Ni | 0.193 | 4.282 | 36.05 |

difference given by $V_{OC}$. The value of the efficiency obtained, considering a 100-$\Omega$ resistive load, which is a good match to the input impedance of a dipole antenna, would be around $1 \times 10^{-9}\%$, which is within the same order of magnitude as the efficiency obtained for antennas coupled to metal-insulator-metal diodes.[6]

From Table 4, it can be seen how the combination of Ti and Ni produces a Seebeck signal that is the largest for the studied combination.

## 4 Conclusions

Responsivity is a key figure of merit in the characterization of optical detection devices. It is defined as the ratio of the output current, or output voltage, and incident optical power. Even though thermoelectric devices based on nanoantennas (Seebeck nanoantennas) have already been proposed as possible energy harvesting devices, until now, no value of their responsivity has been reported. In this work, a numerical evaluation and comparison of the responsivity of three types of Seebeck nanoantennas using different materials and geometries is presented. The geometry analysis shows how the square spiral geometry has the widest bandwidth and the highest induced current of the three geometries. However, the geometry that can generate a higher temperature gradient is the bowtie antenna, which favors the thermoelectric effect in a Seebeck nanoantenna. In addition, the analyzed results show the way to propose improved designs, including optimized geometry and the effect of the surroundings and auxiliary elements.

From the numerical results, it can also be seen that these types of devices can present a voltage responsivity as high as 36 $\mu$V/W for titanium-nickel nanodipoles resonant at far-infrared wavelengths. This value encourages the use of Seebeck nanoantennas as energy harvesters working with thermal radiators at moderate temperatures.

## Acknowledgments

BMV acknowledges the scholarship of the Consejo Nacional de Ciencia y Tecnología (CONACYT), as well as the Universidad de Guadalajara and the Universidad Autónoma de San Luis Potosí for the support to accomplish this research. FJG would like to acknowledge support by project 32 of CEMIE-Solar from Fondo Sectorial CONACYT-Secretaría de Energía-Sustentabilidad Energética and by the National Laboratory program from CONACYT through the Terahertz Science and Technology National Lab (LANCYTT). JA would like to recognize the financial support of the Spanish Ministerio de Economía y Competitividad through project TEC2014-40442.

## References

1. L. Novotny and N. van Hulst, "Antennas for light," *Nat. Photonics* **5**, 83–90 (2011).
2. P. Bharadwaj, B. Deutsch, and L. Novotny, "Optical antennas," *Adv. Opt. Photonics* **1**, 438–483 (2009).
3. F. J. González, "Optical antennas," in *Wiley Encyclopedia of Electrical and Electronics Engineering*, J. Webster, Ed., pp. 1–5, Wiley, New York (2015).
4. E. Briones et al., "Seebeck nanoantennas for solar energy harvesting," *Appl. Phys. Lett.* **105**(9), 093108 (2014).

5. G.P. Szakmany et al., "Nanoantenna integrated infrared thermoelectric converter," in *IEEE 14th Int. Conf. Nanotechnology (IEEE-NANO 2014)*, pp. 571–573 (2014).
6. E. Briones, J. Alda, and F. J. Gonzalez, "Conversion efficiency of broad-band rectennas for solar energy harvesting applications," *Opt. Express* **21**(S3), A412–A418 (2013).
7. G. P. Szakmany et al., "Antenna-coupled single-metal thermocouple array for energy harvesting," in *45th European Solid State Device Research Conf. (ESSDERC 2015)*, pp. 89–92 (2015).
8. R. A. Wood, "Monolithic silicon microbolometric arrays," in *Uncooled Infrared Imaging Arrays and Systems*, P. W. Kruse and D. D. Skatrud, Eds., Vol. **47**, pp. 45–122, Academic Press, New York (1997).
9. A. Cuadrado, J. Alda, and F. J. González, "Distributed bolometric effect in optical antennas and resonant structures," *J. Nanophotonics* **6**, 063512 (2012).
10. F. J. González et al., "The effect of metal dispersion on the resonance of antennas at infrared frequencies," *Infrared Phys. Technol.* **52**, 48–51 (2009).
11. E. D. Palik and G. Ghosh, *Handbook of Optical Constants of Solids*, Academic Press, San Diego (1998).
12. A. Cuadrado et al., "Detectivity comparison of bolometric optical antennas," *Proc. SPIE* **9547**, 954735 (2015).
13. L. Novotny, "Effective wavelength scaling for optical antennas," *Phys. Rev. Lett.* **98**, 266802 (2007).
14. F. J. González and G. D. Boreman, "Comparison of dipole, bowtie, spiral and log-periodic IR antennas," *Infrared Phys. Technol.* **46**(5), 418–428 (2005).

**Brhayllan Mora-Ventura** received his BS degree in communications and electronics engineering in 2010 and his MS degree in 2015. He worked as an engineer at PISA Laboratories in 2011. He obtained a certificate of Black Belt Lean Six Sigma in 2012. He is currently a PhD student at the Universidad Autónoma de San Luis Potosí. His interests include nanophotonics, harvesting of solar energy and analysis, and fabrication of nanostructures. He is a student member of SPIE and OSA.

**Ramón Díaz de León** received his BS degree in electronic engineering and his MS degree in computational sciences from ITSLP, and his PhD in applied sciences from the Autonomous University of San Luis Potosí. He is a professor with the Electric-Electronic-Mechatronic Department, Instituto Tecnológico de San Luis Potosí, México. His research interests include numerical simulation, photonics, optical spectroscopy, and crystal growth.

**Guillermo García-Torales** received his BS degree as an engineer in communications and electronics from the University of Guadalajara in 1989, his PhD was obtained in 2001 from the Centro de Investigaciones en Optica A. C. (CIO). He is a full professor at the Universidad de Guadalajara since 2001. He is a member of the Sistema Nacional de Investigadores (México), the Mexican Academy of Optics, the Mexican Society of Physics, SPIE, and OSA.

**Jorge L. Flores** received his BS degree in electronics engineering from the University of Guadalajara, Mexico, in 1996 and his PhD in optics from Centro de Investigaciones en Óptica, Mexico, in 2001. He is a researcher in the Electronics Department at the University of Guadalajara. His interests include optics sensors and image processing and their applications.

**Javier Alda** graduated in 1985 as a Lic. in sciences from the University of Zaragoza and received his PhD in physics from the University Complutense of Madrid in 1988. He joined the Optics Department of the University Complutense of Madrid in 1985 and he is currently a professor of optics. He has coauthored more than 100 journal publications, 100 communications in international meetings and conferences, and has three patents in optics. He is a fellow of SPIE.

**Francisco Javier González** received his BS degree from ITESO University, Guadalajara, Mexico, in 1996, and his MS and PhD degrees from the School of Optics and Photonics, University of Central Florida in 2000 and 2003, respectively. He is currently a professor at the Autonomous University of San Luis Potosí, San Luis Potosi, Mexico. He has authored or coauthored more than 65 journal papers and holds three patents in the areas of infrared detectors, nanophotonics, and biophotonics.